JOURNAL OF MATERIALS SCIENCE 4 (1969) 997–1002

Electrical and Electron Microscope Observations on Antimony-Implanted Silicon

M. D. MATTHEWS
Solid State Division, AERE, Harwell, Didcot, Berks, UK

Received 15 May 1969

Sheet resistivity and Hall effect measurements have been combined with controlled anodic oxidation and hydrofluoric acid stripping to determine donor distributions with depth and mobilities in antimony implanted silicon (50 and 100 keV, 10^{13} to 3×10^{15} ions/cm^2). The mobilities were found to be similar to those in diffused junctions, but the peak of the donor profile was significantly deeper than expected theoretically. Electron microscopy has been used to investigate unusual effects occurring at the highest doses where the solid solubility (10^{20} atoms/cm^3) was exceeded, giving rise to antimony precipitation together with poor surface recrystallisation on annealing.

1. Introduction

In the design of solid state devices where the doping is achieved by ion implantation, accurate knowledge of the mean range and spread in depth of implanted ions is of vital importance. Also the implantation conditions, e.g. target temperature and orientation, as well as subsequent annealing treatments must be optimised [1]. This paper reports measurements made on silicon crystals implanted with varying doses of antimony ions at room temperature and annealed to minimise the adverse effects of the radiation damage unavoidably introduced. Profiles of electrically active implanted antimony have been determined by combining sheet resistivity and Hall effect measurements with controlled layer removal by anodic oxidation and hydrofluoric acid stripping. Electron microscopy has been used to follow the annealing stages and to interpret unusual electrical effects at high dose levels.

2. Experimental

The antimony ions were implanted at 50 and 100 keV into the polished* surfaces of $\langle 111 \rangle \pm 1°$, 5 to 10 Ω cm p-type silicon crystals. The ion beam was scanned over the whole slice (3.2 cm diameter) giving a uniform dose to within about 5% over the area to be anodically oxidised and $\sim$ 10 to 15% over the entire slice. All implantations were carried out with the target at room temperature and doses of between 10^{13} and 3×10^{15} ions/cm^2 employed. Before measurement, slices were annealed at 650 to 700° C for 30 to 60 min in a vacuum of $\sim 3 \times 10^{-6}$ torr.

The van der Pauw specimen geometry [2] is particularly suitable for Hall and resistivity measurements on ion implanted specimens. A differential analysis enabling both the carrier concentration and mobilty to be calculated as a function of depth beneath the surface has been described by Mayer *et al* [3]. A clover leaf geometry is used to reduce the influence of contacts and, in the present work, was made by masking off the implant using black wax and etching in a mixture of 65% HNO_3 (5 parts), 40% HF (3 parts) and CH_3COOH (3 parts).

Satisfactory electrical contacts were made using gallium-indium paint (3 Ga:1 In by weight) for all but the lowest doses. For doses less than about 5×10^{13} ions/cm^2, the antimony concentration near the surface was very low and low energy, high dose, implanted antimony contacts were preferred. Even so, measurements on these implants were not very accurate due to the low doping levels and very shallow junction depths.

Because the range of 50 to 100 keV antimony

*Polished slices were obtained from Monsanto Chemicals Ltd.

ions (mass 122) in silicon is small and the profile narrow, thin layers of silicon had to be removed between readings. This was carried out by the conventional method of anodically oxidising the silicon to a known depth and stripping the oxide with dilute hydrofluoric acid. An estimate of the oxide thickness used, and hence the thickness of silicon removed, was made from the current density and time of the anodic oxidation using the data of Wilkins [4]. In the case of 100 keV implants, the first oxide thickness to give an interference colour (tan) was used and it was estimated that this resulted in the removal of 168 $\pm$ 20 Å silicon. This figure was checked by weighing which gave 170 $\pm$ 17 Å.

A 2.5 kG permanent magnet was used for the Hall measurements and readings taken for reversal of specimen current and magnetic field.

3. Results

3.1. Annealing Characteristics

Fig. 1 shows plots of sheet resistivity and carrier concentration as a function of isochronal annealing temperature for a specimen implanted with $\sim 10^{15}$ ions/cm^2 at 100 keV. Rapid changes occurred between 550 and 650° C which corresponds to the epitaxial recrystallisation temperature of the amorphous surface film created during room temperature implantation [5]. This change is therefore associated with the removal of damage centres and the movement of antimony atoms to substitutional sites. These conclusions are in agreement with those published by Mayer *et al* [3, 6].

There is apparently no gain in annealing above 650° C. This is so despite the existence of a persistent slight surface colouration (similar to that produced by an amorphous layer), on high dose ($\sim 10^{15}$ ions/cm^2) samples after 650° C anneals. It was concluded at first that this colouration was indicative of residual lattice damage and hence a poor implant. This idea was supported by the fact that these surfaces were etched vigorously by CP4 to give a matt finish. However, it was found that these junctions behaved very well electrically and good profiles and carrier mobilities were obtained. Moreover, the colouration and etching effects were eliminated by removing the first 150 Å of silicon, indicating that a special surface effect was being observed. It was concluded that these effects were being produced by small amounts of antimony which diffuses to form precipitates on or near the surface by virtue of the higher vacancy concentration near the surface during annealing. Because antimony has a high vapour pressure, the surface antimony could be removed by prolonged heating but the silicon oxide inevitably present probably hinders this process.

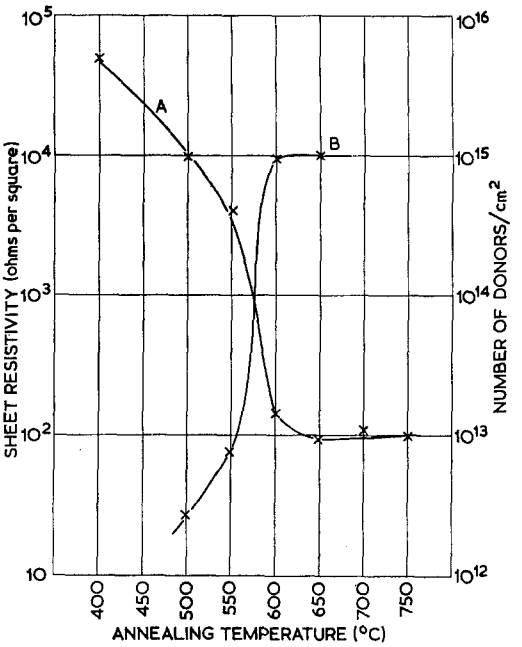

Figure 1 Sheet resistivity (curve A) and carrier concentration (curve B) as a function of isochronal (30 min) annealing temperature for a 100 keV $\sim 10^{15}$ ions/cm^2 specimen.

3.2. Profile and Mobility Measurements

Profiles of electrically active antimony are shown in fig. 2 and the carrier mobilities for several specimens are plotted as a function of carrier concentration in fig. 3. The solid curve in fig. 3 is the mobility variation found in diffused structures taken from the data of Irvin [7]. The difference between the Hall and conductivity mobilities has been neglected as it should be small for the high doping levels used. It is seen that in the implanted structures, as in diffused structures, the mobility is being determined predominantly by impurity scattering and that any scattering by residual lattice defects is insignificant in comparison.

In fig. 2 the profiles have, in fact, been calculated using Irvin's mobility data to reduce the experimental scatter of points given by the differential analysis. These profiles do not have the gaussian shape predicted by the theory of Lindhard *et al* [8] because no effort was made to

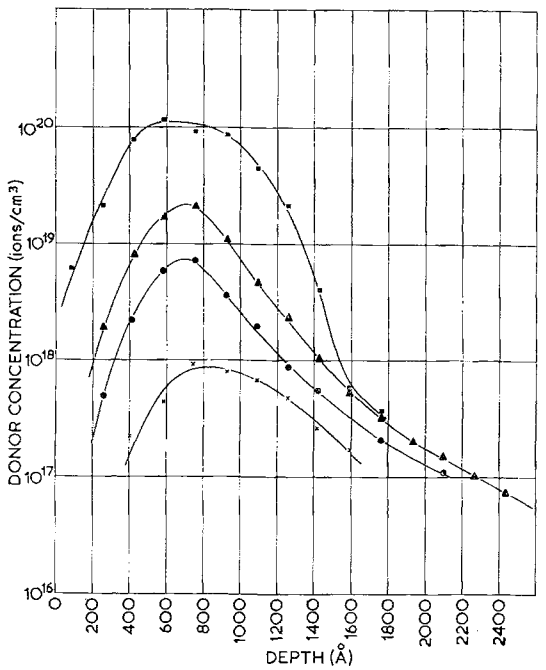

Figure 2 Donor distributions in 100 keV antimony implants at various dose levels after 700° C 30 min anneals. ■, 1.4×10^{15}; ▲, 2.3×10^{14}; ●, 7.0×10^{13}; ×, 1.2×10^{12} ions/cm².

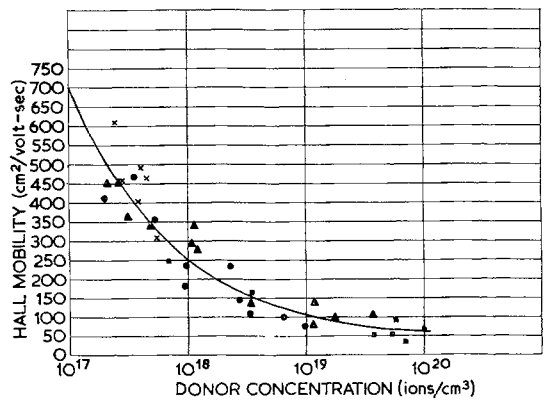

Figure 3 Implanted carrier mobility values as a function of carrier concentration. Solid curve is variation expected for diffused structures where impurity scattering dominates. ■, 1.4×10^{15}; ▲, 2.3×10^{14}; ●, 7.0×10^{13}; ×, 1.2×10^{12} ions/cm².

limit channelling. The critical angle for channelling of 100 keV antimony ions in the ⟨111⟩ directions is about 4°, so there is an appreciable channelled fraction even without accurate beam alignment. Indeed, in the case of the lowest dose, where a complete amorphous surface layer was not formed, the ratio of channelled to random component is seen to be comparable.

The mean range of the higher dose curves was ~ 700 Å which is significantly greater than the 560 Å calculated from Lindhard's results [8] and the 448 Å obtained by Gibbons [9] from computer evaluations of Lindhard's range integrals. If a gaussian curve is fitted to the random component of the profiles, the half width (at $1/e$ of the maximum concentration) was measured to be 260 Å. This should be compared with a value of 176 Å given by Lindhard's results and only 71 Å quoted by Gibbons.

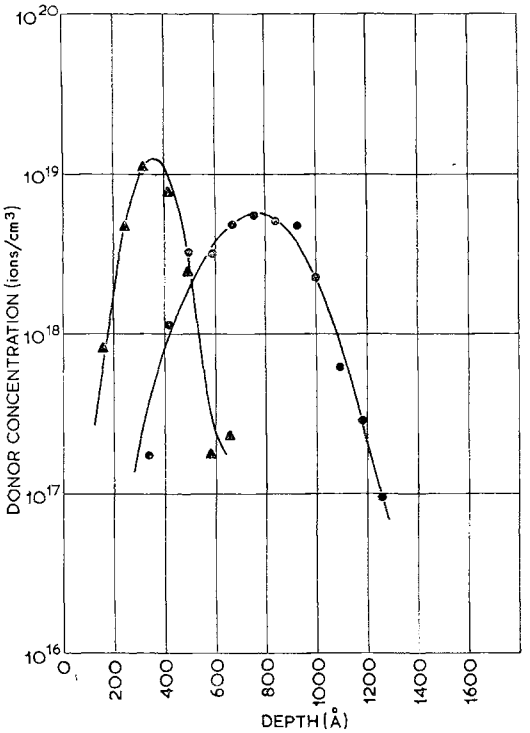

Figure 4 Profiles obtained for a 50 keV and 100 keV implants OMK with channelling minimised. Annealed for 30 min at 700° C.
▲, 50 keV, 7×10^{13} ions/cm²; ●, 100 keV, 7×10^{13} ions/cm².

To carry out a more accurate comparison with theory, channelling must be suppressed. This has been done in fig. 4 where, for the 50 keV implant, the specimen was misoriented from ⟨111⟩ and, for the 100 keV implant, the channels were blocked by a pre-irradiation with argon ions (100 keV, 5×10^{14} ions/cm²). In both cases gaussian profiles were obtained. The half widths (at $1/e$ of the peak value) were measured to be 250 ± 30 and 120 ± 40 Å. It was therefore

concluded that both the mean ranges and standard deviations of the antimony profiles were substantially greater than the values predicted by the best available theories. This is perhaps not so surprising in view of the rather drastic approximations necessary in the theory.

Secondary electron emission from the silicon was not suppressed or monitored during implantation, so it was not possible to obtain an accurate figure for the fracture of implanted atoms which became electrically active. It was estimated, however, that this figure was high, in the range 65 to 85%, by using a secondary electron coefficient measured in separate experiments. The fraction of electrically active ions was not dose dependent.

With reference to fig. 2, it may be seen that the donor distribution for the highest dose (1.4×10^{15} ions/cm^2) was much broader than that found for lower doses. The rather flat top to this profile is explained by the fact that the antimony concentration around the peak exceeded the solid solubility limit ($\sim 10^{20}$ atoms/cm^3). The relevant solubility limit appears to be the maximum value (normally obtained at 1300° C) and not the value corresponding to the annealing temperature used. This is reasonable in view of the non-equilibrium nature of the recrystallisation process and the fact that the whole surface had to be regrown epitaxially giving impurity atoms a chance of taking up desirable substitutional sites. It has previously been shown that the number of electrically active centres in a boron implant is greatly increased if a complete amorphous surface is recrystallised [10]. The increased width of the profile cannot be explained in terms of normal substitutional antimony diffusion which is too slow. It is possible, however, that those atoms which could not adopt substitutional sites owing to the solid solubility being exceeded were able to diffuse by an interstitial mechanism. Bulthuis [11] has proposed an interstitial diffusion mechanism to explain increased penetrations observed in Ga and In implanted silicon. Once these atoms had migrated away from the peak concentration they could move into substitutional sites given a sufficient vacancy concentration. Because amorphous silicon is some 10% less dense than crystalline silicon [5], it is likely that as the recrystallisation occurred a sufficient supply of vacancies was indeed momentarily maintained.

If the antimony concentration was increased still further asymmetrical profiles were obtained

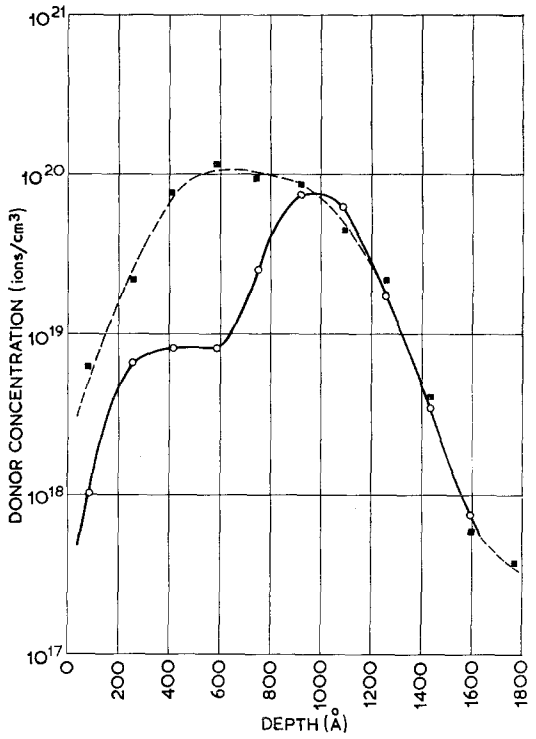

Figure 5 100 keV 2.7×10^{15} ions/cm^2 specimen after 30 min 700° C anneal showing the effects on the profile of exceeding the solubility limit. ■, 1.4×10^{15} ions/cm^2; ○, 2.7×10^{15} ions/cm^2.

(fig. 5). In this case, the solid solubility limit had been exceeded by at least a factor of 2 near the peak. An explanation of this profile was obtained by observing specimens irradiated to different doses in the electron microscope. A sequence of micrographs with the corresponding diffraction patterns is shown in fig. 6. The residual damage was similar in nature in all cases, appearing as complex arrays of small regions of dark contrast. The diffraction patterns revealed that, for the lower doses, a 680° C anneal is more than sufficient to completely recrystallise the surface, and the diffraction patterns contain typical ⟨111⟩ spot patterns. For doses above about 10^{15} ions/cm^2, however, the surface became partially polycrystalline and diffraction rings were observed. For the highest dose the precipitation of a second phase (metallic antimony) could be detected. These observations suggested that when the solid solubility limit was significantly exceeded the excess antimony was able to diffuse and formed small precipitates. The presence of these precipitates interfered with the epitaxial

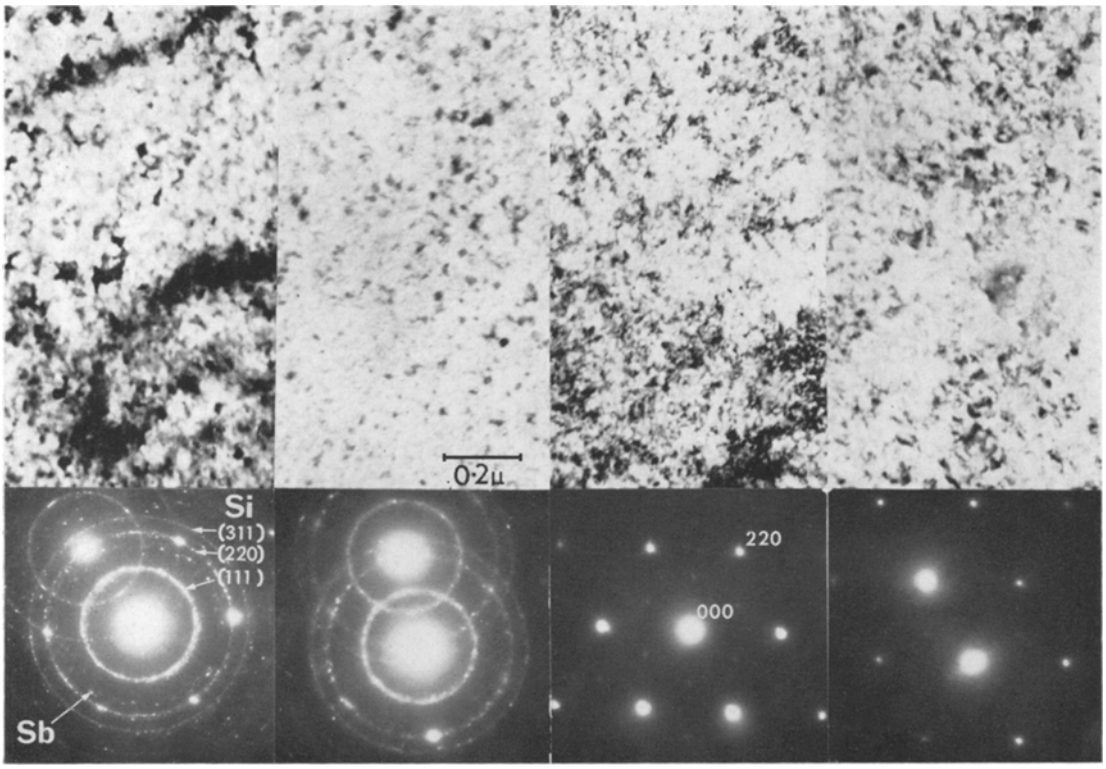

Figure 6 Electron micrographs of a series of specimens implanted with 50 keV antimony ions to different doses and annealed at 680° C for 30 min. Doses (a) 4.3×10^{16}, (b) 8.5×10^{15}, (c) 1.7×10^{15}, (d) 3.4×10^{14} ions/cm^2.

regrowth of the silicon and a partially polycrystalline surface was produced. It is then reasonable to conclude that the profile of fig. 5 could have been produced by the extra damage near the surface trapping some of the carriers. Despite the additional damage, carrier mobilities were not substantially reduced and impurity scattering still dominated.

4. Conclusions

4.1. General Results

The following main conclusions were reached:

(i) The implanted carrier mobilities were determined by impurity scattering and were thus similar to those found in diffused structures.

(ii) The mean projected range and spread in depth of antimony ions in silicon is significantly higher than that predicted by the theory of Lindhard.

(iii) Significant channelling tails were found on profiles of ⟨111⟩ oriented specimens.

(iv) The solid solubility limit of antimony in silicon obtainable in room temperature implants after annealing at 650 to 700° C is $\sim 10^{20}$ atoms/cm^3.

(v) If the solid solubility is significantly exceeded, antimony precipitates form on annealing and the observations suggest that these may interfere with the epitaxial recrystallisation to give a partially polycrystalline surface.

4.2. Comparison with Implants carried out at ~ 500° C

It is interesting to compare the results of the present investigation with profiles obtained by Mayer *et al* [3] for implantations carried out with the targets at ~ 500° C.

There seems to be no significant difference in the number of electrically active antimony atoms obtained for similar doses using the two methods. This is a consequence of the fact that antimony atoms readily take up substitutional lattice sites, and is not a general result applicable to other systems.

The carrier mobilities reported by Mayer for "hot" implants are marginally lower than those

measured in the present work. It is not clear whether this is caused by additional scattering from lattice defects in "hot" implants (where it is known that very dense dislocation arrays exist [5]) or simply due to the proximity of the surface in the case of Mayer's 20 keV implants where the expected mean range is only ~ 120 Å. Much sharper profiles were obtained from room temperature implants. This was due at least in part to the reduced amount of channelling in the present work caused by the rapid accumulation of radiation damage in room temperature implants. In "hot" implantations, on the other hand the surface remains crystalline and the total number of channelled ions is increased. Owing to the very high dynamic vacancy concentration present during "hot" implantations, broadening of the profile may also occur by radiation enhanced diffusion. It is impossible to assess this possibility more precisely in the absence of further information.

Acknowledgement

I would like to thank Dr R. S. Nelson for helpful advice, Miss N. G. Blamires for valuable discussions regarding the experimental technique and Mr R. N. Copp for carrying out the implantations.

References

1. N. R. LARGE and J. H. BICKNELL, *J. Materials Sci.* **2** (1967) 589.
2. L. J. VAN DER PAUW, *Philips Res. Repts.* **13** (1958) 1.
3. J. W. MAYER, O. J. MARSH, G. A. SHIFRIN, and R. BARON, *Can. J. Phys.* **45** (1967) 4073.
4. N. A. WILKINS, AERE Report R.5875.
5. D. J. MAZEY, R. S. NELSON, and R. S. BARNES, *Phil. Mag.* **17** (1968) 1145.
6. L. ERIKSSON, J. A. DAVIES, N. G. E. JOHANSSON, and J. W. MAYER, *J. Appl. Phys.* **40** (1969) 842.
7. J. C. IRVIN, *Bell Syst. Tech. J.* **XLI** 2 (1962) 387.
8. J. LINDHARD and N. SCHARFF, *Phys. Rev.* **124** (1961) 128.
9. J. F. GIBBONS, *Proc. IEEE* **56** (1968) 295.
10. N. G. BLAMIRES, M. D. MATTHEWS, and R. S. NELSON, *Phys. Lett.* **28A** (1968) 178.
11. K. BULTHUIS, *ibid* **27A** (1968) 193.